AIP | Applied Physics Letters

Reduced efficiency roll-off in phosphorescent organic light emitting diodes at ultrahigh current densities by suppression of triplet-polaron quenching

F. X. Zang, T. C. Sum, A. C. Huan, T. L. Li, W. L. Li et al.

Citation: Appl. Phys. Lett. **93**, 023309 (2008); doi: 10.1063/1.2955527
View online: http://dx.doi.org/10.1063/1.2955527
View Table of Contents: http://apl.aip.org/resource/1/APPLAB/v93/i2
Published by the American Institute of Physics.

Reduced efficiency roll-off in phosphorescent organic light emitting diodes at ultrahigh current densities by suppression of triplet-polaron quenching

F. X. Zang,[1,a)] T. C. Sum,[1,a)] A. C. H. Huan,[1] T. L. Li,[2] W. L. Li,[2] and Furong Zhu[3]
[1]*Division of Physics and Applied Physics, School of Physical and Mathematical Sciences, Nanyang Technological University, 21 Nanyang Link, Singapore 637371, Singapore*
[2]*Key Laboratory of Excited State Processes, Changchun Institute of Optics, Fine Mechanics and Physics, Chinese Academy of Sciences, Changchun 130033, People's Republic of China and Graduate School of Chinese Academy of Sciences, Beijing 100039, People's Republic of China*
[3]*Institute of Materials Research and Engineering, 3 Research Link, Singapore 117602, Singapore*

(Received 15 April 2008; accepted 14 June 2008; published online 18 July 2008)

High-performance phosphorescent organic light emitting devices with reduced efficiency roll-off at ultrahigh current densities were realized. The devices were $Ir(ppy)_3$-based phosphorescent organic light emitting diodes that employed 1,3-bis[2-(2,2′-bipyridine-6-yl)-1,3,4-oxadiazo-5-yl]benzene as a high mobility electron transfer layer. The device's brightness was enhanced while the efficiency roll-off was reduced. The device exhibits high current efficiency (21 cd/A) at high brightness (80 000 cd/m^2), with a maximum luminescence of 136 000 cd/m^2 at over 1 A/m^2 (with an efficiency of 13 cd/A). This reduction in efficiency roll-off is attributed to the suppression of the triplet-polaron quenching rate through balancing the charge carrier ratio in the device. © *2008 American Institute of Physics*. [DOI: 10.1063/1.2955527]

Phosphorescent organic light emitting diodes (PhOLEDs) are one of the most promising candidates for next-generation display or lighting applications.[1] These devices exhibit high external quantum efficiencies $\eta_{ext} \sim 20\%$ at low current density.[2] However, a fast reduction of η_{ext} known as roll-off occurs at high current densities. This limits the use of PhOLED in high-brightness applications such as displays, solid-state lighting, or organic lasers. Baldo *et al.*[3] reported that this roll-off is mainly attributed to the triplet-triplet annihilation (TTA) (i.e., ${}_3M^* + {}_3N^* \rightarrow {}_1M + {}_3N^*$) of the long-lived triplet excitons. Recently, Reineke *et al.*[4] demonstrated that the roll-off could also be due to a triplet exciton-polaron (TP) quenching process (i.e., ${}_3M^* + N^- \rightarrow {}_1M + N^{-*}$). The former process scales with the square of the triplet exciton density n_{ex} at high current densities. In contrast, the latter process is dependent on the polaron density in the active areas and scales linearly with n_{ex}. Other contributions to the efficiency roll-off include device degradation, field-induced quenching,[5] etc. Several methods proposed to minimize this roll-off effect include the use of dual emitting layers in PhOLEDs[6] and the use of high-performance fluorescent materials to compensate the reduction in efficiency in the electroluminescence (EL).[7]

Typically, the hole polaron (h^+) population dominates due to the higher hole mobility of hole transfer materials. This causes an imbalance of the charge carriers. A large number of holes and polarons accumulate at the interface and within the device active area, respectively, resulting in TP quenching.[5,8] In light of this, one method to minimize the efficiency roll-off in PhOLEDs would be to counter the imbalance of the charge carrier ratio through the use of suitable high mobility electron transfer materials. A high-electron mobility material will permit more electrons to travel to the active layer. A more balanced charge carrier ratio will facilitate the formation of excitons and reduce h^+ formation, thus reducing the TP quenching rate.

In this paper, we report on the realization of a high-performance $Ir(ppy)_3$-based PhOLED with Bpy-OXD {1,3-bis[2-(2,2′-bipyridine-6-yl)-1,3,4-oxadiazo-5-yl]benzene} as the electron transfer material. This work is a proof of concept that a high mobility electron transfer material could be used in PhOLEDs to suppress the efficiency roll-off at ultrahigh current densities. The device exhibits high current efficiency (21 cd/A) at high brightness (80 000 cd/m^2), with a maximum luminescence of 136 000 cd/m^2 at over 1 A/m^2 (with an efficiency of 13 cd/A). These values are higher than those of the reference devices fabricated under the same conditions.

Figure 1(a) shows the chemical structures of the materials used in the device. All the materials were commercially purchased and used without further purification. Bpy-OXD

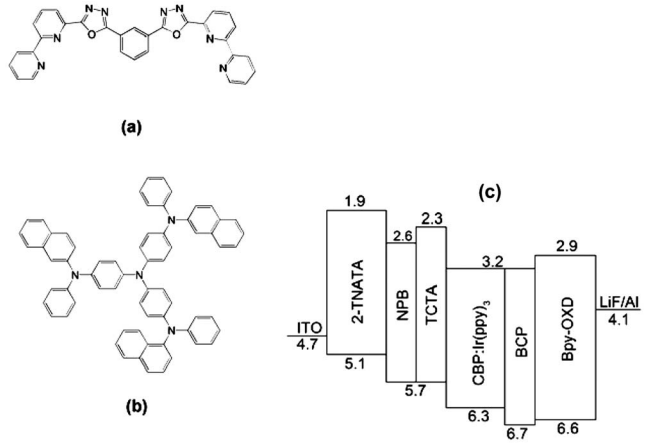

FIG. 1. Chemical structures of (a) Bpy-OXD and (b) 2-TNATA. (c) A schematic of the device configuration.

[a)]Authors to whom correspondence should be addressed. Electronic addresses: fxzang@ntu.edu.sg and tzechien@ntu.edu.sg.

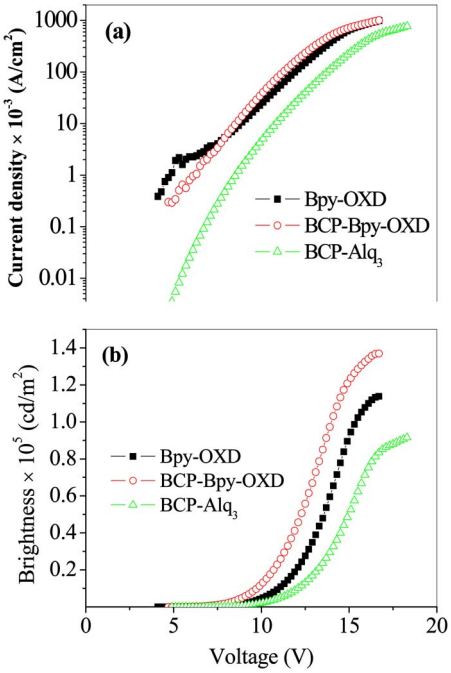

FIG. 2. (Color online) The current-voltage and voltage-brightness relationship of ITO/2TNATA/NPB/TCTA/CBP:Ir(ppy)$_3$ (6%)/ hole block and ETLs (1,2,4)/LiF/Al. (Devices 1: BCP 40 nm; 2: Bpy-OXD 40 nm; 4: BCP/Alq$_3$ 10/30 nm).

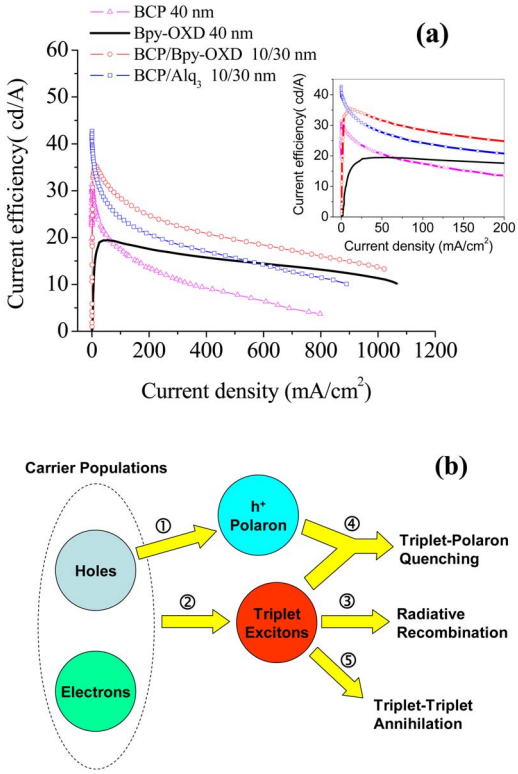

FIG. 3. (Color online) (a) Current density–current efficiency relationship of devices 1–4. The Inset shows a close-up of the initial current density–current efficiency relationship. (b) A schematic illustrating the dynamic interplay between the exciton and h^+ formation processes, and TTA and TP quenching processes.

(an electron transfer material) is an oxadiazole derivative with a high-electron mobility of 10^{-3} cm/V s and a glass transition temperature (T_g) of 106 °C. Its lowest unoccupied molecular orbital (LUMO) and highest occupied molecular orbitals (HOMO) levels are 2.95 and 6.45 eV,[9] respectively. Indium tin oxide (ITO) substrates of 20 Ω/sq were cleaned with detergent and solvent. They were subsequently treated by O_2 plasma for 30 s at 900 W before being loaded into a vacuum chamber for OLED fabrication. Organic films and the cathode were successively deposited onto the substrates by thermal evaporation in a vacuum chamber (at 3 $\times 10^{-4}$ Pa) without breaking vacuum. The evaporating rate was kept at 1–2 Å/s for the organic layers and 5 Å/s for Al, respectively. The active areas of the made-up devices were ~0.04 cm^2. We fabricated a total of four different types of devices and their structures [see Fig. 1(b)] are as follows: ITO/2TNATA {4,4′,4″-tris[*N*-(2-naphthyl)-*N*-phenyl-amino]triphenylamine} (30 nm)/NPB[*N*,*N*′-bis(naphthalen-1-yl)-*N*,*N*′-bis(phenyl)-benzidine] (10 nm)/TCTA[4,4′,4″-tris(*N*-carbazolyl)-triphenylamine] (10 nm)/CBP:Ir(ppy)$_3$ (6%) (30 nm)/hole block and electron transfer layers (ETLs) (1–4)/LiF (0.5 nm)/Al (200 nm). [1: BCP (2,9-dimethyl-4,7-diphenyl-1.10- Phenanthroline) 40 nm; 2: Bpy-OXD 40 nm; 3: BCP/Bpy-OXD 10/30 nm; 4: BCP/Alq$_3$ 10/30 nm.] The 2TNATA/NPB layer is the hole injection and hole transfer layer (HTL) and the TCTA layer is the electron blocking layer. The brightness current voltage (B-I-V) test was performed using a Keithley 2400 sourcemeter and 2000 multimeter coupled to a TOPCON(r) luminance colorimeter BM-7. The spectrum and color coordinates were investigated using a TOPCON luminance colorimeter BM-7.

A comparison of the EL performance and current efficiency among devices 2–4 are given in Fig. 2 The devices that employed Bpy-OXD as the ETL showed a dramatic increase in the current density and brightness compared to those that used BCP/Alq$_3$ (device 4). From Fig. 2(b), the highest brightness achieved in device 3 was 136 000 cd/m^2 at 17.5 V. This value is comparable to the highest reported value.[10] The highest performance of device 4 is ~90 000 cd/m^2 at 18.5 V. Figure 3(a) shows the current density–current efficiency relationship of devices 1–4. The highest current efficiency of device 1 is ~32 cd/A under low current density. Under high current density (>200 mA/cm^2), device 1 shows a drastic reduction in efficiency. Device 3 exhibits the best overall current efficiency and is more durable than the other devices. Its highest current density extends beyond 1000 mA/cm^2 with a corresponding current efficiency of ~13 cd/A at 136 000 cd/m^2. Interestingly, although the initial efficiency of device 3 is smaller than that of device 4, it exhibits less efficiency roll-off than the latter. It is also evident in Fig. 3(a) that using materials with increasing electron mobility ($\mu_{\text{Bpy-OXD}}=4\times10^{-3}$ cm^2 V^{-1} s^{-1} > $\mu_{\text{Alq3}}=5\times10^{-5}$ cm^2 V^{-1} s^{-1} > $\mu_{\text{BCP}}=6\times10^{-7}$ cm^2 V^{-1} s^{-1}) (Refs. 9, 11, and 12) reduces the roll-off at high current density; consistent with the increased EL at high current density as shown in Fig. 2(b).

The inset of Fig. 3(a) shows a close-up of the initial efficiency of the four devices (<200 mA/cm^2). The devices that use Bpy-OXD show a gradual increase in efficiency followed by a peaking of the efficiency at the low current density (~11 mA/cm^2). In contrast, other devices exhibit the highest efficiency at the onset of current application. Their efficiency rapidly decreases as the current densities increase. These observations are a consequence of a dynamic interplay between the radiative exciton recombination, TTA, and TP processes. This can be explained using a simple illustration shown in Fig. 3(b) with devices 3 and 4 as a comparison (while operating under the same current densities).

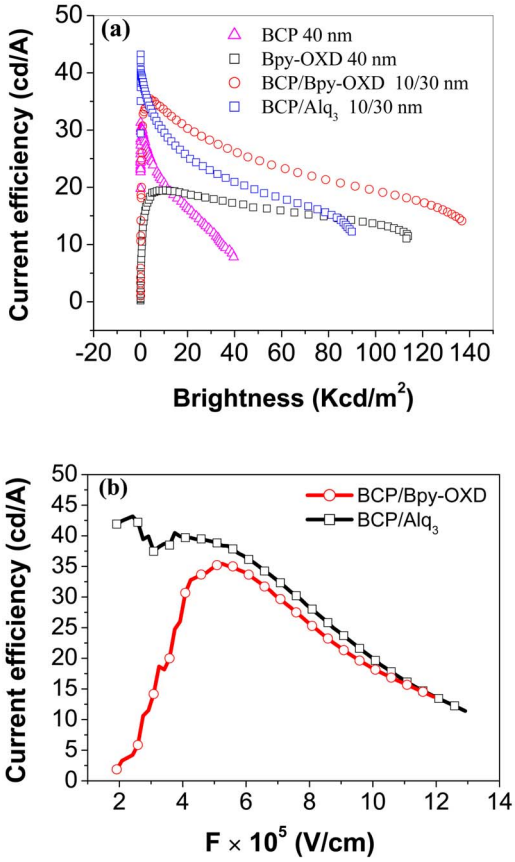

FIG. 4. (Color online) (a) Luminescence–current efficiency curve of devices 1–4. (b) Graph of the current efficiency–electric field relationship for device **3** (BCP/Bpy-OXD) and device 4 (BCP/Alq_3).

In device 3, the high-electron mobility Bpy-OXD layer allows more electrons into the active layers, thus balancing the charge carrier ratio. This reduces the formation of h^+ polarons [1—see Fig. 3(b)] and increases the formation of excitons (2). Upon increasing current densities, TP quenching (4) is gradually reduced due to the smaller h^+ population, while TTA (5) is increased relatively (compared to TP) due to the increased n_{ex}. This phenomenon gives rise to the peak at ~11 mA/cm^2. The increased n_{ex} also results in enhanced EL (3) from device 3. Beyond 11 mA/cm^2, TTA (5) could possibly play a more dominating role. The efficiency roll-off is thus reduced with the suppression of TP quenching (4).

In device 4, Alq_3 has a lower-electron mobility compared to Bpy-OXD. The imbalance of charge carriers facilitates h^+ formation (1). Under the same applied current densities as device 3, relatively fewer electrons are transported to the active areas in device 4. Hence, there is a relatively lower rate of exciton formation (2) and a higher rate of h^+ formation (compared to device 3). Upon applying voltage, the effect of TTA is small because of the low n_{ex}. Hence, device 4 exhibits the highest current efficiency at the onset. The effects of both TP quenching (4) and TTA (5) are always present. Unlike device 3, the h^+ population in device 4 is not suppressed. The contributions from both 4 and 5 result in a faster decrease in the current efficiency.

Figure 4(a) shows the luminescence–current efficiency curve. The devices that use Bpy-OXD give a relatively high device durability that can reach over 1 A/cm^2, and EL performance that are over 110 000 cd/cm^2. For devices 2, 3, and 4, at a luminance of 10 000 cd/m^2, efficiencies of 29, 34, and 20 cd/A were achieved, respectively. At a luminance of 80 000 cd/m^2, efficiencies were lowered to 15, 21, and 14.8 cd/A, respectively. This shows that the current efficiency is increased with an increase in the material's electron mobility.

Another important contribution to efficiency roll-off that should be considered is the effects of the field-induced exciton quenching.[5] The dc electric field, F, in an OLED can be estimated.[8] $F = U/d_{in} - U_{bi}/d_{in}$, where U_{bi} is the built-in potential and d_{in} is the thickness of the intrinsic layers. The built-in potential is determined from the difference between the LUMO of ETL and the HOMO of HTL. Since the values of the LUMO for Alq_3 and Bpy-OXD almost match (i.e., 3.00 and 2.95 eV, respectively) and that devices 3 and 4 have the same thicknesses, F is not expected to be very different when operating under the same voltage. From Fig. 4(b), the current efficiencies of devices 3 and 4 are rather similar under high F. Beyond a field of 5.5×10^5 V/cm, under the same F, the current efficiency of device 3 is slightly lower than that of device 4. This shows that the effects of field-induced exciton quenching are not affected by the increase in exciton density. Further research is needed to determine the degree of the contributions from TTA, TP quenching, and field-induced exciton quenching to the efficiency roll-off.

In summary, high-performance $Ir(ppy)_3$-based PhOLEDs with Bpy-OXD as the electron transfer material were realized. The device exhibits high current efficiency (21 cd/A) at high brightness (80 000 cd/m^2); with a maximum luminescence of 136 000 cd/m^2 at over 1 A/m^2. This work shows that the high mobility ETL in PhOLEDs reduces the efficiency roll-off at ultrahigh current densities. This is due to the suppression of the TP quenching rate through balancing the charge carrier ratio in the device. The dynamic interplay between the various processes is explained. Further work to probe the charge carrier and exciton dynamics using field assisted pump-probe and time-resolved electroluminescence spectroscopy are currently in progress.

This work is supported in part by a grant (042 101 0014) from the Agency for Science, Technology and Research (A*STAR), Singapore. The authors are extremely grateful to Dr. Zhu Furong for the fruitful discussions and contributions to this work.

[1] M. A. Baldo, D. F. O'Brien, Y. You, A. Shoustikov, S. Sibley, M. E. Thompson, and S. R. Forrest, Nature (London) **395**, 151 (1998).
[2] C. Adachi, M. A. Baldo, M. E. Thompson, and S. R. Forrest, J. Appl. Phys. **90**, 5048 (2001).
[3] M. A. Baldo, C. Adachi, and S. R. Forrest, Phys. Rev. B **62**, 10967 (2000).
[4] S. Reineke, K. Walzer, and K. Leo, Phys. Rev. B **75**, 125328 (2007).
[5] J. Kalinowski, W. Stampor, and J. Mezyk, Phys. Rev. B **66**, 235321 (2002).
[6] G. He, M. Pfeiffer, K. Leo, M. Hofmann, J. Brinstock, R. Pudzich, and J. Salbeck, Appl. Phys. Lett. **85**, 3911 (2004).
[7] Y. Sun, N. C. Giebink, H. Kanno, B. Ma, M. E. Thompson, and S. R. Forrest, Nature (London) **440**, 04645 (2006).
[8] D. Hertel and K. Meerholz, J. Phys. Chem. B **111**, 12075 (2007).
[9] M. Ichikawa, T. Kawaguchi, K. Kobayashi, T. Miki, K. Furukawa, T. Koyama, and Y. Taniguchi, J. Mater. Chem. **16**, 221 (2006); M. Ichikawa, N. Hiramatsu, N. Yokoyama, T. Miki, S. Narita, T. Koyama, and Y. Taniguchi, Phys. Status Solidi (RRL) **1**, R37 (2007).
[10] M. A. Baldo, S. Lamansky, P. E. Burrows, M. E. Thompson, and S. R. Forrest, Appl. Phys. Lett. **75**, 4 (1999).
[11] K. Itomo, H. Ogawa, and Y. Shirota, Appl. Phys. Lett. **72**, 636 (1998).
[12] C. Hosokawa, H. Tokailin, H. Higashi, and T. Kusumoto, Appl. Phys. Lett. **60**, 1220 (1992).